HEAT TRANSFER BEHAVIOR OF A HIGH TEMPERATURE STEEL PLATE COOLED BY A SUBCOOLED IMPINGING CIRCULAR WATER JET

Hormando Leocadio [a], Julio Cesar Passos [b], Antonio Fabio C. da Silva [c]

(a) Maintenance Engineering Division, Usiminas, Brazil, hormando.leocadio@usiminas.com
(b) Mechanical Engineering Department/LEPTEN/Boiling, UFSC, Brazil, jpassos@emc.ufsc.br
(c) Mechanical Engineering Department - SINMEC - UFSC, Brazil, afabio@sinmec.ufsc.br

ABSTRACT

Impingement water jets are used as a fast cooling system (≈ 85°C/s) for hot steel plates, because of the high extracted heat flux (≈ 10 MW/m^2). The microstructure and mechanical properties are dependent on the controlled cooling in the run-out table hence it is important to obtain an accurate heat transfer coefficient value.

This paper presents an experimental and numerical study on the heat transfer behavior of a high temperature steel plate cooled by a subcooled impinging circular water jet. The effects of the surface temperature on the heat transfer regimes were analyzed by the transient inverse heat conduction method to calculate the heat flux on the impinging surface from the temperatures measured with thermocouples inserted in square steel plates.

The results showed that the water jet will be in direct contact with the surface even if the temperature (600 to 900°C) exceeds the boiling temperature and also that the heat transfer regime is not single-phase. The water jet can be in contact with a hot strip surface without the formation of a vapor film, with strip traveling at 10 m/s. The results will contribute to a better understanding of the heat transfer regimes during hot strip mill cooling.

INTRODUCTION

Many industrial applications use free impingement jets, because of the high rates of heat transfer that can be obtained using relatively simple equipment [1]. Run-out table temperature control is one of the most important processes in terms of ensuring mechanical properties and obtaining the desirable grain structure of a steel strip [2]. For a hot strip mill the finishing and coiling temperatures are in the ranges of 800-950°C and 510-750°C, respectively. In order to reduce the strip temperature at the exit of the last stand in the finishing train to the coiling temperature, the strip is mainly cooled by the cooling water on the run-out table [3], as shown in Fig. 1. This involves internal and external conduction, forced convection, forced boiling convection, air convection, radiation and heat generation from material phase transformation.

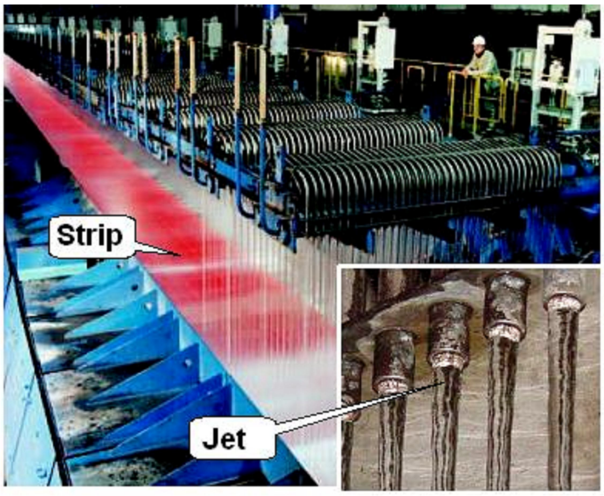

Figure 1: Hot strip mill cooling system built at Severstal using circular water jet in Cherepovets, Russia in 2003.

The entire heat transfer mechanism is still not fully understood because involves a complex mixture of the phenomena of water impinging and boiling on a surface moving at around 10 m/s [4].

In the literature, authors disagree regarding the heat transfer regime that occurs in the impingement zone during cooling in a hot strip mill. According to Prieto and Menendez [5], in the impact zone the regime is single-phase forced convection, even with surface temperatures of 600°C < T_s < 900°C, but they do not explain how to evaluate water properties at 1 atm beyond the saturation point. Viskanta and Bergman [6] and Timm et al. [7] describe a transition regime due to the high heat flux and surface temperature. From their visual observations, Zumbrunnen et al. [2] described the regimes that occur during the cooling of a hot strip mill as showed in Fig. 2.

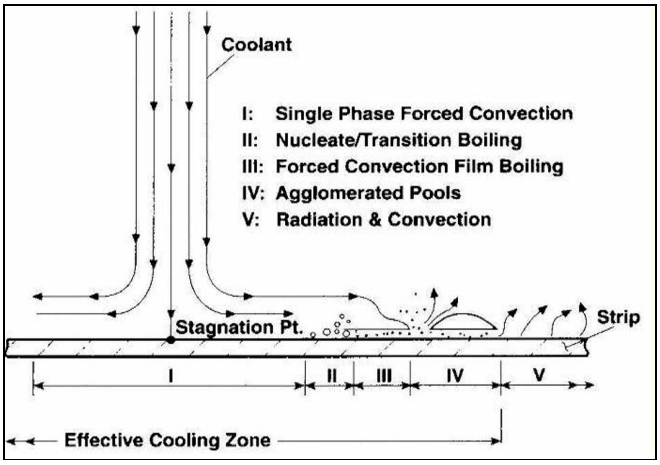

Figure 2: Heat transfer regimes adjacent to impingement planar water jet on hot strip [2].

In Zone I the heat transfer is single-phase forced convection, and the surface temperature is below the saturation temperature. In Zone II there is the nucleate boiling regime in a narrow range and in Zone III film boiling appears. Once the film boiling begins, there is a disordered state on the hot surface of the plate, shown in Zone IV.

Ochi et al. [8] and Leocadio [9] et al. showed that subcooling affects strongly the heat flux and prevents the formation of the film in the impinging zone. Results published by different authors [4, 10] show divergent heat transfer coefficient values.

The purpose this study is to contribute to the understanding of the regimes occurring during the cooling of a high temperature plate due to an impinging circular water jet on a steel plate heated to 600, 750 and 900°C using the experimental apparatus constructed at the Research Center of USIMINAS Steel Plant, in Brazil. The effects of the surface temperature on the heat transfer regimes were analyzed using a 2D axisymmetric finite element method based transient inverse heat conduction model was used to back-calculate the heat flux and heat transfer coefficients along the impinging surface of a plate from the temperatures measured using thermocouples inserted in square hot steel plates. The results will contribute to a better understanding of the heat transfer regimes during a hot steel plate cooling at high temperatures.

MATERIAL AND PROCEDURE

Experimental Facilities

The Figure 3 shows the outline of the experimental facilities installed at the Research Center of USIMINAS Steel Plant, in Brazil. The coolant fluid is the ordinary city water stored in a tank (16), with an equivalent pressure head of 7 m, allowing an exit flow jet (13) at the end of U-tube (14) (curvature radius of 70 mm; inner diameter of nozzle exit D_n = 10 mm). A U-tube (14) is is used in order to keep the water from the nozzle in the state of a stable flow without including air at the nozzle exit and to be compatible with those used in the steel industry. The overflow tube (1) has the function of keeping the water level in the water tank (16) constant, ensuring a constant pressure in the U-tube.

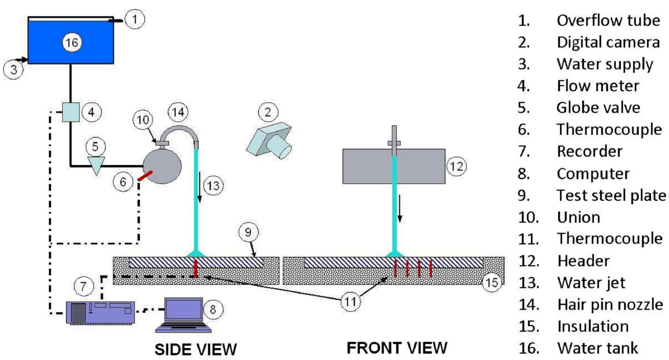

Figure 3: Outline of the experimental apparatus.

The steel plate (9) was heated to the test temperature in a 75 kW electrical furnace 800 mm wide, 1000 mm long and 600 mm high which can heat up to 1300°C. The plate material was AISI 304 in order to prevent oxidation and phase transformation during the cooling process, as occurs with carbon steel shown in Fig. 4. The square plate dimensions were 150 mm length and 10 mm thickness.

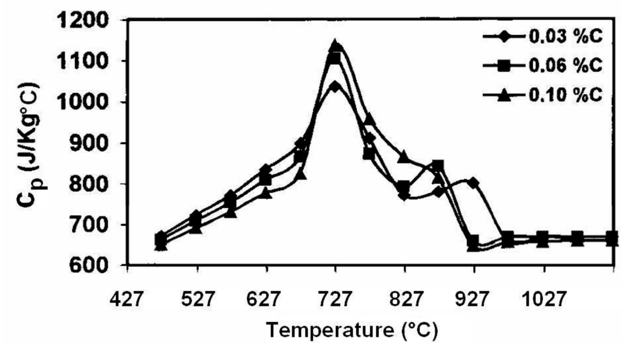

Figure 4: Vary of specific heat for carbon steel with the temperature [5].

Table 1 shows some properties of AISI 304 for temperatures between 27 and 927°C [11]. On the sides of the plate without impingement insulation was used with conductivities of 0.17 $W/m^2.°C$ (1090°C) and 0.078 $W/m^2.°C$ (540°C), and 50 mm thickness. The data acquisition system, with 10 channels, allows an acquisition rate of 10 points per second. The flow rate of the water jet was Q_n = 6 ℓ/min measured using a flow meter with an error of ±0.25%.

Table 1: Thermo-physical properties for AISI 304 [11].

T (°C)	c_p (J/kg°C)	ρ (kg/m^3)	k (W/m°C)
27	447	7900	15.2
127	515	7859	16.6
327	557	7774	19.8
527	582	7685	22.6
727	611	7582	25.4
927	640	7521	28.0

Experimental Procedure

The plate temperature profile during cooling was measured by means of thermocouples inserted into the plate. The K-type thermocouples (11) with a diameter of 1.5 mm were mounted aligned at r distances from the central point of 0, 15, 35 and 55 mm at height, y, of 10 mm from the bottom of the plate. They were heated in an electrical furnace up to the test temperature and transferred to the test position. The cooling process was started at test temperatures of 600, 750 and 900°C. The height of the water jet exit, H, was set at 300 mm and inner diameter of nozzle exit, D_n, was 10 mm. The water jet temperature was 22°C, measured using a K-type thermocouple (6) inside the header (12). When the experimental results were numerically analyzed, the air temperature was assumed to be constant 25°C. The sides of the plate without impingement were assumed to be adiabatic because heat loss on this surface was lower than on the impingement surface. A digital camera was employed to capture images during the cooling process at a rate of 13 photos per seconds (intervals of 0.08 seconds).

Figure 5-a shows a photograph of a circular water jet of 6 ℓ/min, from the nozzle exit at H = 300 mm, on the plate surface. The incident jet diameter, D_j = 6.8 mm, is smaller than the jet at the nozzle exit, D_n = 10 mm, because of the increase in kinetic energy as a function of the jet approximation to the impingement surface. In the stagnation zone there is pressure and vertical velocity, V_j. Outside this zone there is the radial flow zone where V_j = 0. Some authors [8, 13] have arrived at a value close to $r / D_j \approx 1.0$ for definition of the stagnation zone diameter, D_{est}. The dimensions of the stagnation zone were evaluated through a photograph of the water jet, as shown in Fig. 5-b.

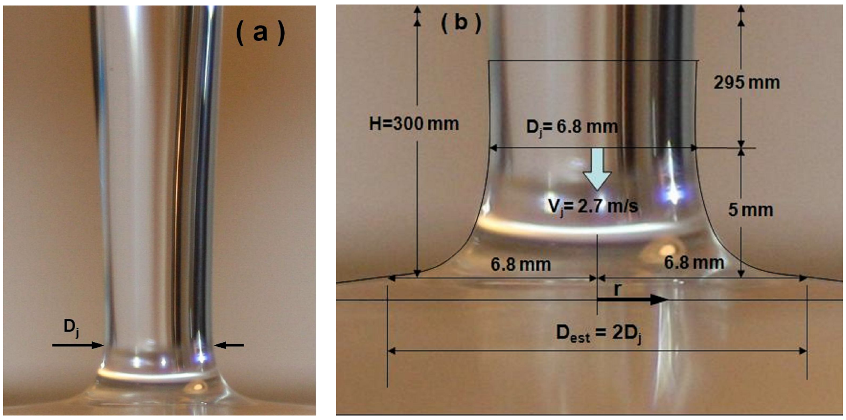

Figure 5: photographs of a circular water jet impinging on the plane surface showing (a) the D_j position and (b) stagnation zone parameters.

Some hydrodynamic parameters are required in heat transfer analysis: impingement jet velocity (V_j), impingement jet diameter (D_j) and saturation temperature at the stagnation point (T_{sat}). These parameters are listed in Table 2 and they were calculated using the continuity and Bernoulli equations. In Ipatinga city, Brazil, where all tests were carried out, the height above sea level is 234 m and the atmospheric pressure is P_{atm} = 95,154 Pa. The stagnation pressure, P_j, represents the active pressure in the collision area the water jet and this pressure is higher than P_{atm}. For V_j = 2,7 m/s the stagnation pressure is P_j = 98,792 Pa and the saturation temperature T_{sat} = 99.3°C. Although, in the hot strip mill cooling process $V_j \approx$ 7 m/s in the stagnation zone which raises the saturation temperature, T_{sat}, to 105.2°C.

Table 2: Hydrodynamic parameters in the stagnation zone.

Q_n (ℓ/min)	D_n (mm)	V_n (m/s)	D_j (mm)	V_j (m/s)	P_j (Pa)	T_{sat} (ºC)
6.0	10	1.3	6.8	2.7	98,792	99.3

Numerical inverse heat conduction analysis

An inverse heat conduction program, developed by Trujillo at Trucomp Co [12], was used to calculate the heat flux on the impinging surface from the measured hot plate temperatures. Tab. 1 shows the thermo-physical properties that are dependent on the temperature for this calculation. A 2D axisymmetric finite element model has been used for the numerical analyze. The model has 75 mm radius, 14 mm thickness and 4200 quadratic elements with 4-nodes per element, as shown in Fig. 6.

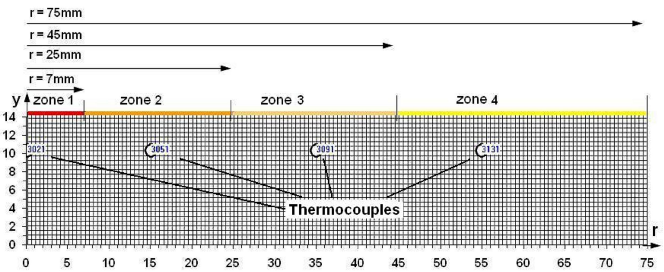

Figure 6: 2D axisymmetric finite element model divided into four surface monitoring zones of heat flux according to the thermocouple positions.

For the boundary conditions, an adiabatic condition was used on the three sides of the plate without impingement, since the quantities of radiative and free convective heat transfer on those surfaces are much lower than the on the impinging side. The top surface of the square plate of 150 mm was divided into four zones with uniform heat flux in each zone: r_1 = 0 to 0.007 m, r_2 = 0.007 to 0.025 m, r_3 = 0.025 to 0.045 m and r_4 = 0.045 to 0.075 m.

RESULTS AND DISCUSSION

Visual analysis

Figure 7 shows successive stages during the cooling process with an initial plate temperature of 900ºC. The digital camera captures the images during the cooling process with intervals of 0.08 seconds.

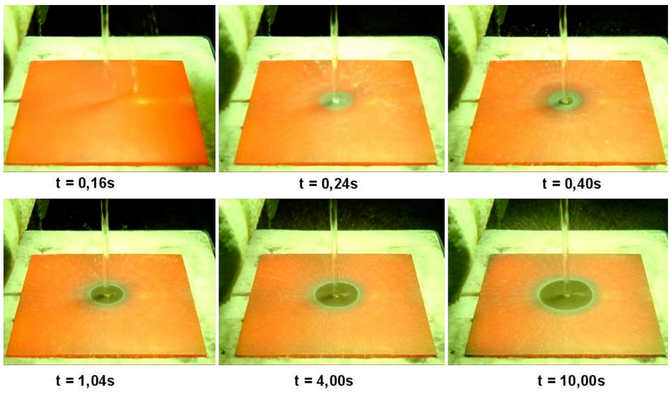

Figure 7: Photographs from cooling process for T_i = 900°C.

After the cooling process started a small white disk appeared at time t = 0.24 s. It disappeared and a dark zone around which a white ring developed. Over time it was observed that the growth rate of the dark zone decreased. The dark zone shows that water is in direct contact with the surface of the plate.

Figure 8 shows sketches illustrating the first steps of the cooling process for the photograph shown in Fig. 7. In Fig. 8-a, the film boiling separates the liquid from heated surface, where there will be a low heat flux.

In Fig. 8-b the jet breaks the boiling film and touches the plate surface, where the temperature is above the Leidenfrost point and there will be a high heat flux. The Fig. 8-c shows the advancement of the wet front which increases over time.

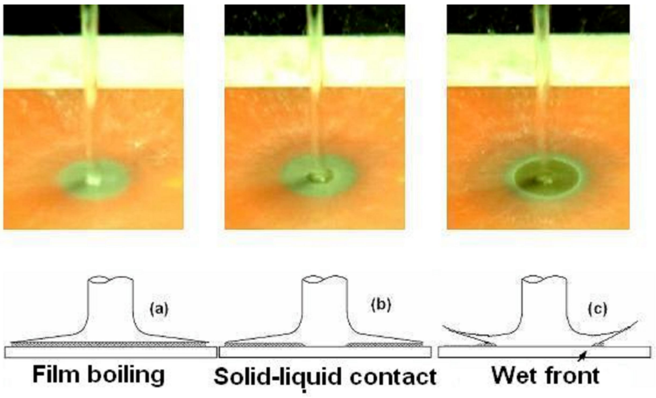

Figure 8: Sketches illustrating the first moments of the cooling stages shown in Fig. 7.

Figure 9 shows, graphically, the growth of the dark zone diameter against time for the initial test temperatures (T_i) of 600, 750 and 900°C. The graph shows that in the first moments, t < 0.8 s, the initial test temperature has a weak influence on the wetting. For t > 1.0 s, the surface temperature has a great influence on the wetting slowing the growth of the wet front.

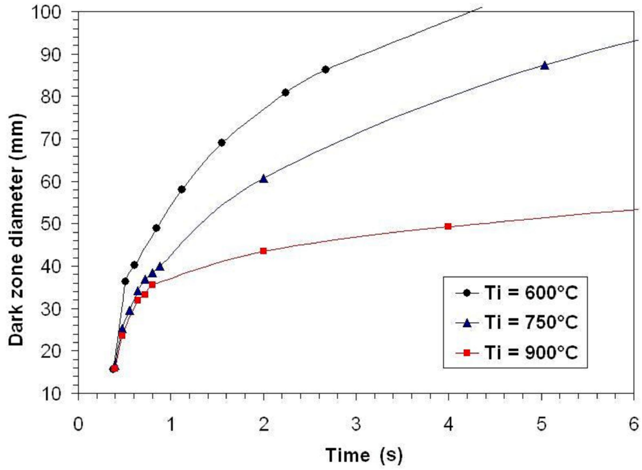

Figure 9: Growth curves of the dark zone diameter as function of time for T_i = 600, 750 and 900°C.

Cooling curves

Figure 10-a shows the cooling curves obtained from the thermocouples 1 to 5, at r = 0, 15, 35, 55 and 75 mm, as seen in Fig. 7.

The cooling process started at instant t = 148 s and the internal temperature was 900°C. The temperature drop was more evident for curve 1, r = 0, where the cooling was more intense. As the dark diameter increases the cooling is intensified in the other curves. Using the inverse heat conduction analysis the surface temperatures were calculated from temperatures inside the test plate (Fig. 10-b) at position r = 0. It was observed that the surface temperature falls faster than the internal temperature in the first seconds at the beginning of the cooling process indicating a highly nonlinear temperature profile inside the plate. These trends also were observed in tests with T_i = 600 and 750°C.

The Fig. 11 shows the nonlinearity inside the plate through the isotherms 16.8 s from beginning of cooling. At impingement point for r = 0 and y = 14 mm, has a temperature of 156°C while for y = 0 the temperature is approximately 624°C.

Analysis of the visual observations in Fig. 7 and the surface cooling curves from the test plate in Fig. 12 revealed that the subcooled water is in direct contact with the superheated surface even when this temperature exceeds, by far, the water saturation temperature. There is no film boiling between the hot surface of the metal and the impinging water jet.

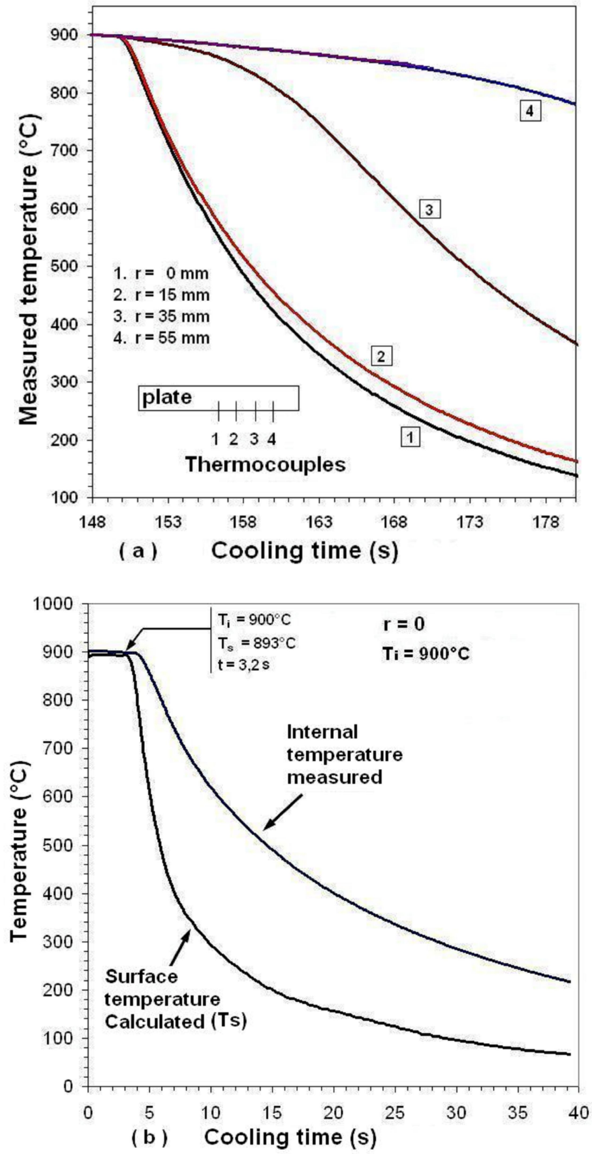

Figure 10: (a) Measured internal temperatures at “r” positions of the radial distance from the center of the plate; (b) Calculated surface and measured internal temperature at r = 0 at stagnation point.

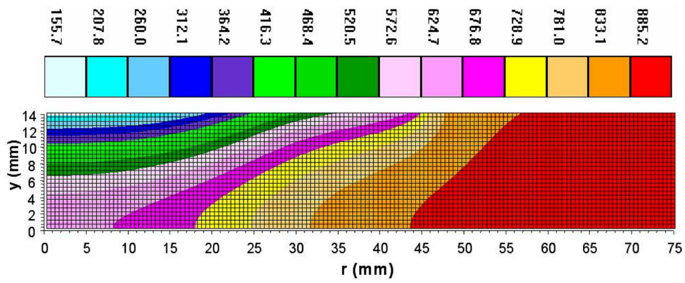

Figure 11: Isothermals at t = 16.8 s after start cooling process for T_i = 900°C.

The time between the beginning of the cooling process and the appearance of the dark zone was approximately Δt = 0.2 s. When Δt = 0.4 s the surface temperature was T_s = 877°C and

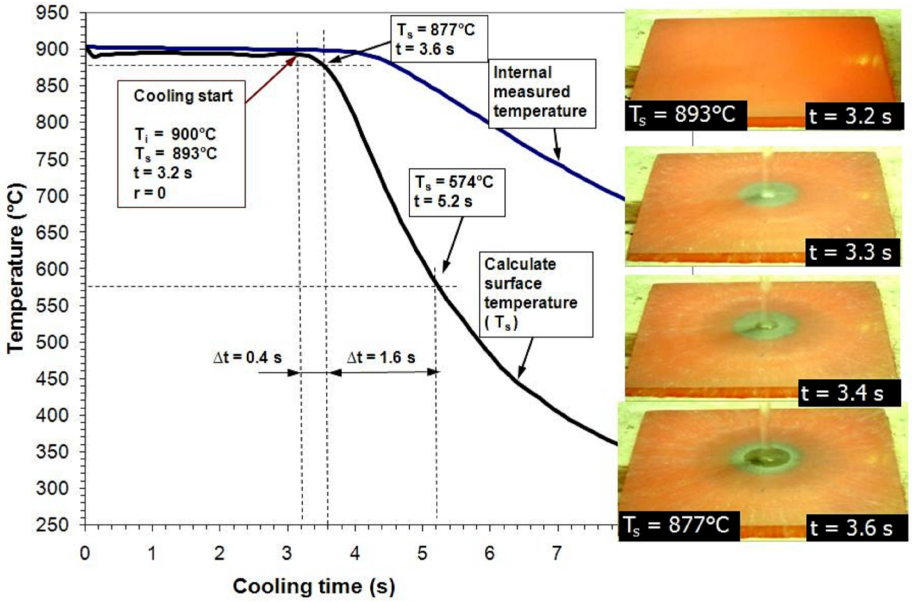

Figure 12: Analysis of the visual observations with the surface cooling curves for T_i = 900°C.

for Δt = 2.0 s T_s = 574°C. In the impact zone there was an absence of bubbles and film boiling. The water jet penetrates the vapor layer and the bubbles formed on the hot surface condense in the subcooled liquid [6, 7]. For the water jet temperature T_j < 60°C, the wetting occurs when the water jet touches the superheated surface, regardless of its temperature [8].

Boiling curves

The Fig. 13-a shows the heat flux curve at r = 0 for T_i = 900°C. The curve can be divided into three regions: single phase forced convection, nucleate boiling and transition. The critical heat flux value, CHF = 3MW/m^2 at T_s = 506°C, is three times greater than the value for pool boiling. The in single phase regime occurs when $T_s \approx$ 140°C. These results indicate that the subcooled and forced convection strongly affects the boiling curve, consistent with the analysis carried out by Robidou et al. [14]. The heat transfer coefficient increases even after the heat flux reaching the CHF. The transition regime is between 506°C < T_s < 893°C. Therefore, for the surface temperatures of T_s = 877 and 574°C, shown in Fig. 12, in the dark zone, the heat transfer regime is transition. This conclusion is consistent with the comments of Timm et al. [3] but contradicts the statements of Hatta et al. [15].

Figure 13-b shows that an increase in the initial test temperature (T_i) promotes an increase in the CHF. For T_i = 600, 750 and 900°C the CHF occurs at T_s = 340, 365 and 506°C, respectively. However, T_i does not affect the beginning of the single-phase and nucleate boiling regimes. For all tests, the single-phase has begun by $T_s \approx$ 140°C and after the CHF all curve have the same declivity.

Figure 14 shows the effect of the initial temperature on the heat transfer coefficients, in the stagnation zone, for T_i = 600, 750 and 900°C. The heat transfer coefficient in the transition region is strongly affected by T_i until $T_s \approx$ 300°C, where the curves meet and remain together until the $T_s \approx$ 50°C, through single phase forced convection and nucleate boiling.

Figure 15 shows the calculated heat flux in the stagnation

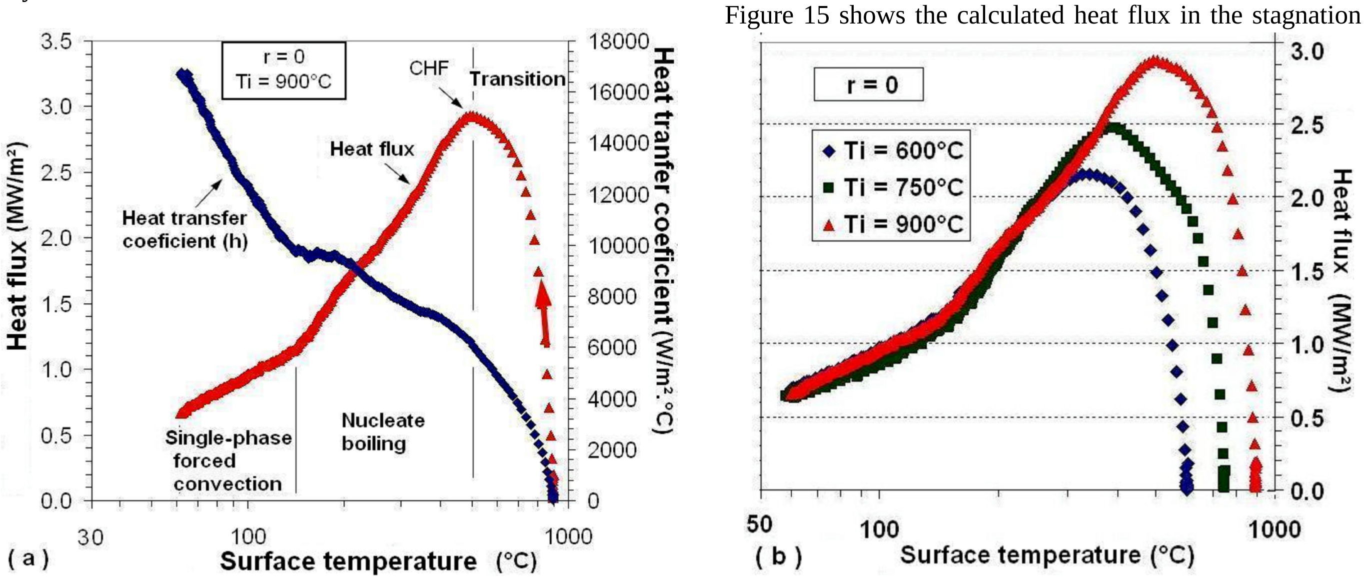

Figure 13: (a) Heat flux and heat transfer coefficient curves at r = 0 for T_i = 900°C and (b) initial test temperature influence on heat flux curve.

zone and in zones 2, 3 and 4, as shown in Fig. 6, for the initial test temperature T_i = 600°C. The time intervals between the CHF increase over time.

The CHF peaks observed in the curves are due to the arrival of the wet front. The CHF peaks decrease as they move away from the stagnation zone. This reduction is due to the in the subcooling of the water and this trend was observed in all tests.

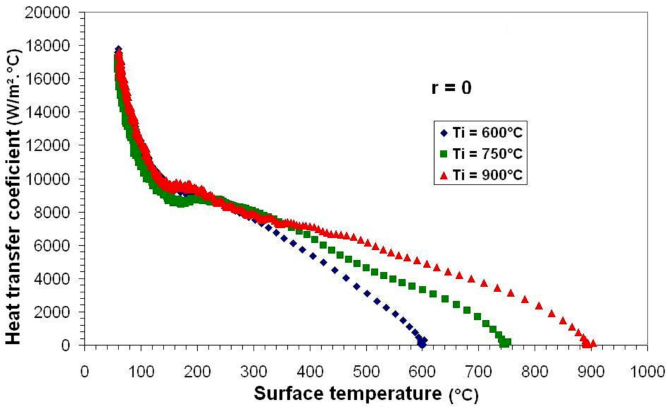

Figure 14: The influence of the initial test temperature on heat transfer coefficient for T_i = 600, 750 and 900°C at r = 0.

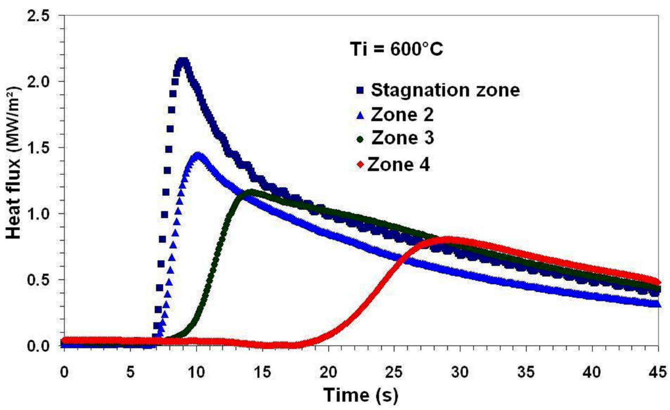

Figure 15: Boiling curves as a function of the time for T_i = 600°C.

Heat transfer during hot strip mill cooling

The Fig. 16 shows a photograph of a water curtain impinging on the hot strip mill at 10 m/s and $T_s \approx$ 900°C where the dark zone can be seen.

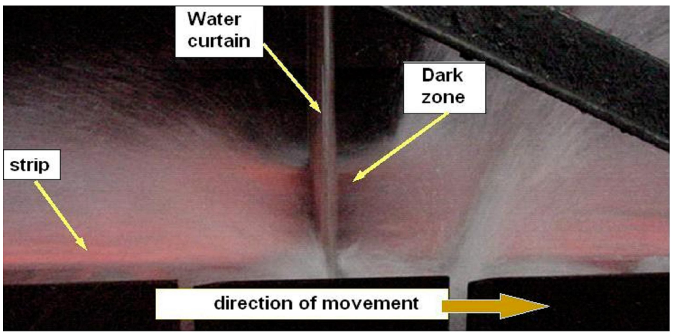

Figure 16: Photograph of a water curtain impinging on the hot strip mill at 10 m/s and $T_s \approx$ 900°C where the dark zone can be seen.

The time that the steel strip remains under the water jet is of the order of thousandths of a second. This is not sufficient to reduce the strip surface temperature of 900°C to a temperature below the saturation temperature, where the single-phase regime could occur, as shown in the graph and photographs of Fig. 12. According to Zumbrunnen et al. [2], during the hot strip mill cooling the regime is single-phase forced convection in the impact region and the surface temperature is below saturation temperature, as shown in Fig. 2.

CONCLUSION

The characterization of the heat transfer during cooling of a high temperature stainless steel plate by an subcooled impinging circular water jet was successfully performed using an experimental apparatus:

1. The surface temperature has a considerable influence on the growth of the dark zone. A higher surface temperature will delay the advance of the wet front.
2. In the impingement zone, r = 0, the CHF value increases with a higher the initial test temperature.
3. The initial test temperature does not affect the single-phase and nucleate boiling curves.
4. The heat flux and CHF are higher in the stagnation zone than in other zones because of greater subcooling of the impinging water jet in the stagnation zone.
5. The subcooled water is in direct contact with the superheated surface even when this temperature exceeds, by far, the water saturation temperature. There is no film boiling between the hot surface of the metal and impinging water jet. The heat transfer regime is not single-phase due to high surface temperature and high heat fluxes.
6. During the controlled cooling in the hot strip mill the surface temperature is far above the water saturation temperature, T_{sat}. The transition regime is likely to occur, contrary to some authors [2, 5, 15] who have considered this region as a single-phase. Therefore, it is not appropriate to use single phase correlations as suggested by Hatta et al. [15] and Prieto and Menendez [5].

The subcooled boiling process in the cooling of high temperature steel plate is complex, requiring research through high speed photos and analysis of the water jet incidence on a surface in motion.

ACKNOWLEDGEMENTS

The authors are grateful for the support of the CNPq, and Hot Rolling Division, Research Center and Maintenance Engineering Division, Usiminas, for providing the test samples, design and assembly of the experimental apparatus and financial support.

NOMENCLATURE

Latin symbols

c_p: Specific heat of test plate (J/kg°C)
CHF: Critical heat flux (MW/m^2)
D_n: Nozzle exit diameter (mm)
D_j: Impinging jet diameter (mm)
D_{est}: Stagnation zone diameter (mm)
H: Height of the water jet exit (mm)

k: Thermal conductivity of test plate (W/m°C)
P_{atm}: Atmospheric pressure (Pa)
P_j: Stagnation pressure (Pa)
Q_n: Water flow at nozzle exit (ℓ/min)
r: Radial distance (mm)
t: Time (s)
T: Temperature (ºC)
T_i: Initial temperature test of plate (°C)
T_j: Impinging water jet temperature (°C)
T_s: Surface temperature (°C)
T_{sat}: Saturation temperature (°C)
V_j: Impinging water jet velocity (m/s)
V_n: Nozzle water velocity (m/s)

Greek symbols
ρ: Density of test plate (kg/m^3)

REFERENCES

1. P. Lee, H. Choi and S. Lee, The Effect of Nozzle Height on Cooling Heat Transfer from a Hot Steel Plate by an Impinging Liquid Jet, Iron and Steel Institute of Japan International ISIJ, v. 44, n° 4, pp. 704–709, 2004.
2. D. A. Zumbrunnen, F.P. Incropera, R. Viskanta, A method and apparatus for measuring heat transfer distributions on moving and stationary plates cooled by a planar liquid jet, *Experimental Thermal and Fluid Science*, v. 3, n° 2, pp. 202-213, 1990.
3. C. J. Barros, H. P. Luna, B. R. Menezes, Study of Applied Models for Hot Strip Mill Cooling Control, Master thesis, Federal University of Minas Gerais, Belo Horizonte, Brazil, 1995.
4. J. Filipovic, R. Viskanta, F.P. Incropera, T. A. Veslocki, Cooling of a Moving Steel Strip by an Array of Round Jets, *Steel Research*, v.65, n° 12, pp.541-547, 1994.
5. M. M. Prieto, L. S. Menendez, Thermal performance of numerical model of hot strip mill runout table, *Ironmaking and Steelmaking*, v. 28, nº 6, pp. 474-480, 2001.
6. R. Viskanta, T. Bergman, *Heat Transfer in Materials Processing, Handbook of Heat Transfer*, cap. 8, 3ª edition, McGraw-Hill, USA, 1998.
7. W. Timm, K. Weinzierl, A. Leipertz, Heat transfer in subcooled jet impingement boiling at high wall temperatures, *International Journal of Heat and Mass Transfer*, v. 46, pp. 1385 - 1393, 2003.
8. T. Ochi, S. Nakanishi, M. Kaji, S. Ishigai, Cooling of a hot plate with an impingement circular water jet, *Multi-Phase Flow and Heat transfer III. Part A: Fundamentals*, pp. 671-681, Elsevier, Amsterdam, 1984.
9. H. Leocadio, A.F.C. Silva, J. C. Passos, Analysis of the cooling effect of a water jet on a hot steel plate, *Proceedings of 19th International Congress of Mechanical Engineering*, Brasília, DF, 2007.
10. F. Xu, M. S. Gadala, Heat transfer behavior in the impingement zone under circular water jet, International *Journal of Heat and Mass Transfer*, Vol. 49, pp. 3785–3799, 2006.
11. F.P. Incropera, D. P. De Witt, *Fundamentals of Heat and Mass Transfer*, 5th Edition, Rio de Janeiro, 2003, 494 p.
12. D.M. Trujillo, H.R. Busby, *INTEMP - Inverse Heat Transfer Analysis - User's manual*, TRUCOMP CO., FOUNTAIN VALLEY, CA, 47 p.,2003.
13. B. W. Webb, C. F. Ma, *Single-phase jet impingement heat transfer*, *Advances in heat transfer*, v. 26, pp. 105-217, Academic press, San Diego, 1995.
14. H. Robidou, H. Auracher, P. Gardin, M. Lebouché, Controlled cooling of a hot plate with a water jet, *Experimental Thermal and Fluid Science*, v. 26, pp.123–129, 2002.
15. N. Hatta, J. Kokado, H. Takuda, J. Harada, J. Hiraku, Predictable Modeling for Cooling Process of a Hot Steel Plate by a Laminar Water Bar, *Archiv für das Eisenhüttenwesen*, v.55, n°4, pp. 143-148, 1984.